CORRECTED 13 JANUARY 2026; SEE LAST PAGE

SCIENCE ADVANCES | RESEARCH ARTICLE

OCEANOGRAPHY

Constraining biorecalcitrance of carboxyl-rich alicyclic molecules in the ocean

Ruanhong Cai[1,2], Oliver J. Lechtenfeld[3]*, Zhenwei Yan[1], Yuanbi Yi[1], Xiaoxia Chen[2], Qiang Zheng[2], Boris P. Koch[4,5], Nianzhi Jiao[2], Ding He[1,6]*

Marine dissolved organic matter (DOM) is one of Earth's largest long-term carbon reservoirs, critical to the global carbon cycle. A key breakthrough in understanding this pool is the identification of biorefractory carboxyl-rich alicyclic molecules (CRAM). Recent studies have challenged the biorecalcitrance of CRAM but lacked detailed molecular evidence. Using advanced online countergradient liquid chromatography–Fourier transform ion cyclotron resonance mass spectrometry to track microbial incubation, we revealed a wide spectrum of CRAM bioavailability regulated by molecular polarity. CRAM with lower polarity were preferentially degraded, whereas microbial reworking led to production of higher-polarity CRAM, characterized by increased oxidation state, nitrogen content, and aromaticity. Some microbially transformed CRAM were frequently detected in a global DOM dataset of 1485 seawater samples, suggesting their potential persistence in marine environments. This study provides molecular insights into the biorecalcitrance and transformation pathway of CRAM, underscoring the complexity and dynamic nature of marine organic carbon cycling.

INTRODUCTION

Marine dissolved organic matter (DOM) holds more than 660 Pg of long-lived reduced carbon, playing a critical role in the global carbon cycle (*1*–*3*). Most of this carbon resists rapid biological decomposition and is widely recognized as recalcitrant DOM (RDOM) (*3*). Advances in modern analytical technologies, particularly ultrahigh-resolution Fourier transform ion cyclotron resonance mass spectrometry (FT-ICR-MS) coupled with soft electrospray ionization, have greatly deepened our understanding of marine DOM. To date, nontargeted direct infusion FT-ICR-MS (DI-FT-ICR-MS) has become a preferred method for analyzing DOM. This approach not only efficiently generates high-resolution molecular fingerprints of DOM but has also been effectively combined with various techniques and geochemical parameters to investigate DOM's origin (*4*–*7*), spatial distribution and pool sizes (*8*–*10*), residence time (*11*, *12*), biorecalcitrance (*13*–*15*), and degradation/removal processes (*10*, *16*) in the ocean. However, the vast structural diversity of DOM (*17*, *18*) poses a major challenge, leaving many RDOM compounds unidentified using conventional DI-FT-ICR-MS (*17*, *19*). This limitation hampers a comprehensive understanding of RDOM cycling and fate in the ocean. Such insights are vital to unraveling how the tremendous marine RDOM reservoir is structured and replenished, particularly with respect to how it responds to future global changes (*20*, *21*).

Using DI-FT-ICR-MS coupled with high-field nuclear magnetic resonance spectroscopy, a distinctive group of DOM compounds was identified, characterized by a complex mixture of carboxylated and fused alicyclic structures. This group was first termed carboxyl-rich alicyclic molecules (CRAM) by Hertkorn *et al.* (*22*). CRAM are widely distributed throughout seawater and have become a frequently referenced RDOM proxy in laboratory incubations (*5*, *23*–*27*) and field studies (*13*, *14*, *28*–*33*). However, the biorecalcitrance of CRAM has recently been questioned (*34*–*36*). As a subfraction of oceanic DOM, CRAM likely represent a continuum of reactivity rather than a discrete molecular class (*11*, *12*). This suggests that CRAM may encompass a variety of molecules with differing properties leading to variable degrees of biological recalcitrance, a hypothesis that is challenging to address with DI-FT-ICR-MS analysis.

Recent advancements in ultrahigh-resolution mass spectrometry have enabled its online coupling with liquid chromatography (LC), substantially enhancing the detection and sensitivity of DOM analysis (*9*, *37*–*42*). Combined with an isocratic elution step and a countergradient, LC-FT-ICR-MS enables the separation of complex DOM compounds according to their polarity prior to FT-ICR-MS measurements, providing crucial insights into the highly polar fractions of DOM (*43*, *44*). As recently demonstrated, polarity plays a critical role in determining the bioavailability of natural DOM compounds in freshwater ecosystems (*45*). This revelation inspires the application of polarity-based LC-FT-ICR-MS analysis to investigate the bioavailability of marine DOM. Compared to conventional DI-FT-ICR-MS, which acquires a single spectrum of mass peaks for a DOM sample, LC-FT-ICR-MS yields multiple spectra across chromatographically defined DOM fractions. This capability allows for a more detailed examination of DOM composition and transformations, offering new insights compared to DI-FT-ICR-MS. Therefore, LC-FT-ICR-MS holds great promise for testing hypotheses regarding the recalcitrance of RDOM, including the biorecalcitrance of specific components, for example, CRAM.

In this study, we applied LC-FT-ICR-MS, following the protocol established by Han *et al.* (*43*), to a 90-day microbial incubation experiment of a coastal seawater (CSW) amended with a diatom intracellular organic matter (DIA) and a coastal sediment-derived DOM (SED). The DIA and SED incubations represent organic matter inputs from the sunlit and the benthic layers. We tracked molecular composition of solid phase extracted DOM (SPE-DOM) at the beginning

[1]Department of Ocean Science, Center for Ocean Research in Hong Kong and Macau, The Hong Kong University of Science and Technology, 999077 Hong Kong SAR, China. [2]State Key Laboratory of Marine Environmental Science, Xiamen University, 361102 Xiamen, China. [3]Department of Environmental Analytical Chemistry, Research Group BioGeoOmics, Helmholtz Centre for Environmental Research–UFZ, Permoserstraße 15, 04318 Leipzig, Germany. [4]Alfred-Wegener-Institut Helmholtz Zentrum für Polar- und Meeresforschung, D-27570 Bremerhaven, Germany. [5]University of Applied Sciences, An der Karlstadt 8, 27568 Bremerhaven, Germany. [6]State Key Laboratory of Marine Pollution, City University of Hong Kong, 999077 Hong Kong SAR, China.
*Corresponding author. Email: dinghe@ust.hk (D.H.); oliver.lechtenfeld@ufz.de (O.J.L.)

and end of the 90-day incubations using LC-FT-ICR-MS (Fig. 1), enabling us to uncover the nuanced DOM composition and its transformations driven by heterotrophic microbial activity. This approach allowed us to verify the bioavailability of subfractions of marine DOM, particularly CRAM, which are often masked by the extreme complexity of DOM.

RESULTS AND DISCUSSION

Microbial transformation of low-polarity SPE-DOM into high-polarity DOM compounds

LC-FT-ICR-MS chromatographically separated DOM along the decreasing polarity of each microbial-incubated DOM sample (*43*). Here, we use the terms "high polarity" and "low polarity" as synonyms for "water-soluble" and "methanol-soluble," respectively. For each 1-min LC segment, the total assigned intensity (TAI) was calculated by summing the intensities of all assigned DOM formulae. These LC fractions were then combined to reconstruct TAI chromatogram for each incubation sample (Fig. 2). The distributions of TAI for the CSW-0-day, DIA-0-day, and SED-0-day incubations were different (Fig. 2), primarily because the DIA and the SED introduced varying qualities of allochthonous DOM compounds into the CSW (CSW-0-day). Notably, the DIA introduced a fraction of low-polarity DOM compounds into the CSW-0-day incubation, as indicated by the high TAIs observed in the LC segments corresponding to 16 to 18 min (Fig. 2 and fig. S1, A to C). Compared to the CSW-0-day incubation, these lower-polarity DOM compounds uniquely contributed by the DIA contained more than 50% aliphatic and fatty acid–like components (fig. S1D), which are typically recognized as biologically labile DOM compounds in the ocean (*10*, *46*). This finding suggests that phytoplankton-derived labile DOM compounds predominantly exhibit lower polarity, which aligns with a recent study showing that bacteria preferentially degrade low-polarity DOM derived from dead-wood leachates (*47*). Consequently, low-polarity DOM likely contributes a relatively large fraction to labile organic components in aquatic environments.

After 90 days of microbial incubation, a similar TAI distribution across the nine LC segments was observed for the CSW-90-day, DIA-90-day, and SED-90-day incubations (Fig. 2), indicating that heterotrophic microbes followed a consistent pattern in transforming DOM (*26*, *48*) and increasing SPE-DOM polarity. The latter is evidenced by the higher TAIs observed in the later LC fractions (retention times of 16 to 19 min) in all 0-day incubations, whereas the maximum TAI shifted to earlier retention times (13 to 17 min) in all 90-day incubations (Fig. 2). Furthermore, compared to the 0-day incubations, a greater number of DOM formulae were assigned to the earlier LC-eluted fractions in all 90-day incubations (fig. S2A). Although the overall TAI of the SED-90-day incubation was lower than that of other 90-day incubations, this discrepancy in TAI magnitude likely results from variations introduced during sample extraction or ionization and does not undermine the observed trend of microbes consistently increasing SPE-DOM polarity over time. Overall, this shift in TAIs across all three incubations after 90 days suggests that heterotrophic microbes preferentially used relatively low-polarity DOM to produce higher-polarity DOM compounds.

Microbes produced high-polarity SPE-DOM with apparently recalcitrant molecular characteristics

Compared to the 0-day incubations, the early eluting DOM (relatively polar; fig. S2A) of the 90-day incubations exhibited higher averaged oxygen to carbon ratios (O/C_a), a higher aromaticity index (AI_a), double bond equivalents (DBE_a), and an increased abundance of CRAM-like formulae but lower H/C_a values (fig. S2, B to F). These parameters have been previously validated as reliable indices for evaluating the biorecalcitrance of DOM samples analyzed by DI-FT-ICR-MS (*49*). Elevated O/C_a, AI_a, and DBE_a and abundance of

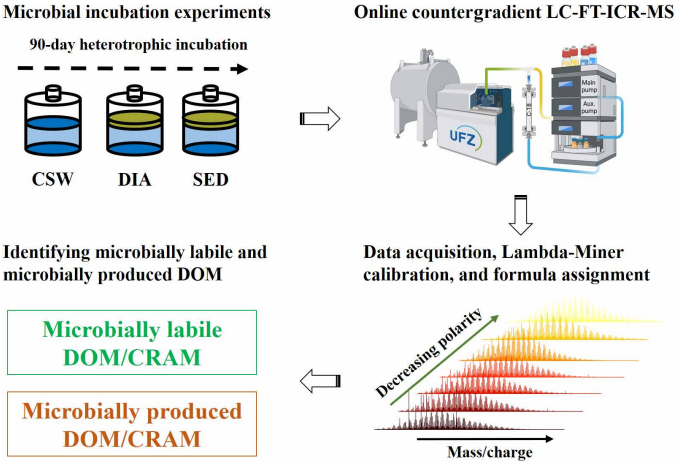

Fig. 1. Schematic workflow for the analysis of microbial-incubated DOM samples using advanced LC-FT-ICR-MS and data processing. The study involved a 90-day incubation experiment to investigate molecular transformation of DOM in coastal seawater (CSW) and this seawater amended with diatom intracellular organic matter (DIA) and coastal sediment-derived DOM (SED). Samples were analyzed using online countergradient LC-FT-ICR-MS. The resulting mass spectrometry data were calibrated using the "Lambda-Miner" tool and processed for DOM formula assignment. Assigned DOM formulae were further categorized as microbially labile and microbially produced DOM, including components such as CRAM.

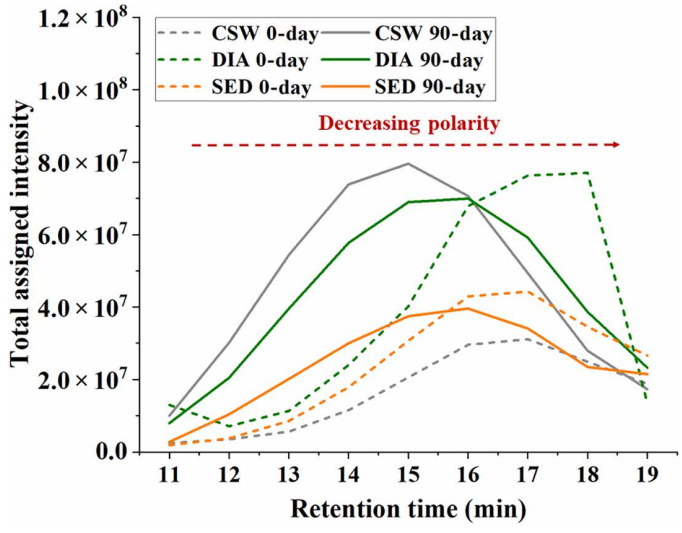

Fig. 2. TAI distribution for 0- and 90-day incubations of CSW, DIA, and SED. A retention time range of 11 to 19 min was selected from each LC-FT-ICR-MS measurement as this range corresponded to the maximum intensity in the total ion chromatograms. The increasing retention time reflects the decreasing polarity of the eluted DOM fractions.

CRAM-like formulae but decreased H/C_a have also been observed in bulk SPE-DOM samples collected from the deep ocean and long-term incubation (*10*, *24*, *26*, *50*, *51*) and related to biologically refractory molecular characteristics. Our experimental findings highlight the microbial production of RDOM in the more polar fractions of SPE-DOM. A recent study revealed that hydrophilic DOM compounds extracted via reverse osmosis represent some of the most biologically labile components in freshwater ecosystems (*45*). This observation does not contradict our findings because our molecular analyses focused on SPE-DOM extracted from seawater. Freshwater DOM generally contains a higher abundance of bioavailable DOM compared to seawater DOM (*52*). Furthermore, reverse osmosis exhibits markedly higher DOM extraction efficiency than solid phase extraction (*53*) and can inherently recover high-polarity DOM compounds such as free amino acids and certain modified carbohydrates. These compounds are labile to microbial degradation (*54*–*56*) and cannot be effectively retained by solid phase extraction (*57*). Therefore, we emphasize that the observed linkage between DOM polarity and bioavailability should be interpreted within the context of SPE-DOM.

To consolidate the evaluation of DOM bioavailability in relation to its molecular polarity, we further identified formulae uniquely present in the 0-day incubation as microbially labile DOM and those emerging in the 90-day incubation as microbially produced DOM (hereafter termed labile and produced DOM, respectively; Fig. 3). Identifying labile and produced DOM formulae using LC-FT-ICR-MS is more robust compared to DI-FT-ICR-MS, as LC-FT-ICR-MS inherently reduce matrix effects commonly occur in DI-FT-ICR-MS analysis (*43*, *58*). Nevertheless, residual matrix effects may still persist. This inherent limitation, along with the use of a signal-to-noise ratio threshold for molecular formula assignment, may interfere the classification of both labile and produced DOM subsets. This identification of labile and produced DOM in each LC segment allowed us to observe a small fraction of DOM molecules that were biologically labile in the earlier eluting LC segments of the CSW, DIA, and SED incubations (fig. S3). These two groups of DOM formulae exhibited distinct chemical properties (Fig. 3). Specifically, the labile highly polar DOM (typically eluting at retention times of 11 to 15 min) in the three incubations consistently exhibited higher H/C_a but lower O/C_a, AI_a, DBE_a, and average molecular mass (m/z_a). In contrast, the produced highly polar DOM was characterized by lower H/C_a and higher O/C_a, AI_a, DBE_a, and m/z_a values across all three incubations. Given that variations in these DOM parameters have been empirically linked to DOM bioavailability under laboratory incubation conditions (*24*, *49*), these experimental results robustly demonstrate that microbes preferentially used labile DOM compounds. Some of these labile compounds may undergo microbial reworking to produce RDOM compounds, particularly within the highly polar fraction of SPE-DOM.

A comparison of the 0- and 90-day DOM samples analyzed using LC-FT-ICR-MS (this study) with the same samples previously analyzed by DI-FT-ICR-MS (*26*) revealed a generally similar van Krevelen distribution (figs. S4 to S6). However, the LC-FT-ICR-MS methodology demonstrates a greater capability for detecting produced DOM molecules, which are typically of high polarity (figs. S4 to S6). In addition, LC-FT-ICR-MS enables the acquisition of detailed molecular insights into both labile (figs. S7A, S8A, and S9A) and produced DOM (figs. S7B, S8B, and S9B) across a gradient of decreasing polarity in these three incubations. For instance, a noticeable decrease in O/C ratios was observed along the gradient of decreasing polarity for both labile and produced DOM (figs. S7 to S9). This observation of the O/C and its connection to microbial transformation of DOM warrants further investigation. These molecular characteristics, which were obscured in DI-FT-ICR-MS analyses, became evident with LC-FT-ICR-MS, providing valuable insights into the molecular properties that influence the bioavailability of DOM and the selective transformation of DOM by microbial activity. Overall, these findings suggest that microbial oxidation under laboratory conditions leads to the production of highly polar RDOM within the SPE-DOM fraction.

CRAM exhibit various degrees of bioavailability

We further identified both microbially labile and produced CRAM from the microbially labile and produced DOM formulae, respectively (Fig. 4). This identification confirms that the widely used RDOM proxy, CRAM, includes biologically labile compounds. Figure 4 illustrates that labile CRAM were predominantly eluted in the later LC segments (retention times of 15 to 19 min), corresponding to the low-polarity constituents of SPE-DOM. This phenomenon is particularly evident in the DIA and SED incubations (Fig. 4, B and C), likely due to the contribution of diatom- and sediment-derived DOM, which introduced additional labile CRAM into incubations. These findings further emphasize the importance of incorporating polarity into DOM bioavailability assessments. Consistent with the bulk SPE-DOM transformation results (Fig. 3 and fig. S3), a small fraction of highly polar CRAM (retention times of 11 to 15 min; Fig. 4) was also identified as labile molecular formulae. However, the formula count for this fraction was consistently smaller than the CRAM produced in the same LC segments across the three incubations (Fig. 4). The labile CRAM were characterized by relatively high H/C and low O/C ratios (Fig. 5, A to C), indicating that they were less oxidized and relatively saturated. DOM with these chemical characteristics is known to be preferentially used by heterotrophic microbes (*11*, *12*, *59*). In contrast, the produced CRAM in the incubations exhibited lower H/C and higher O/C ratios (Fig. 5, D to F). A consistent trend was observed between labile and produced CRAM molecular formulae when analyzed excluding heteroatoms (N, S, and P; fig. S10). These trends suggest that microbial activities produce CRAM with more oxidized and less saturated chemical characteristics.

Following the original definition of CRAM (*22*), CRAM-like formulae with high intensities fall within a specific enclosed region in the van Krevelen diagrams (Fig. 5). Compared to the labile CRAM (Fig. 5, A to C), microbes produced more highly polar CRAM, which occupied the remaining area (lower right) of the enclosed region (Fig. 5, D to F). Within this framework, CRAM located in the upper left of the enclosed region, characterized by lower polarity, exhibited relatively high biolability, whereas those in the lower-right area, with higher polarity, consisted of more recalcitrant compounds. The produced CRAM formulae exhibited significantly higher values of AI_a, DBE_a, and averaged nominal oxidation state of carbon ($NOSC_a$) than the labile CRAM formulae ($P < 0.0001$, t test; Fig. 6). Elevated AI and DBE values indicate an increased presence of aromatic structures in DOM molecules (*60*). Furthermore, a higher NOSC value suggests a relatively oxidized carbon state and lower Gibbs energy in the molecules (*61*). These findings suggest that the produced CRAM contain more aromatic structures in their carbon backbones and likely more carboxyl groups in their side chains. Should this occur, microbial reworking of CRAM may increase their aromaticity and

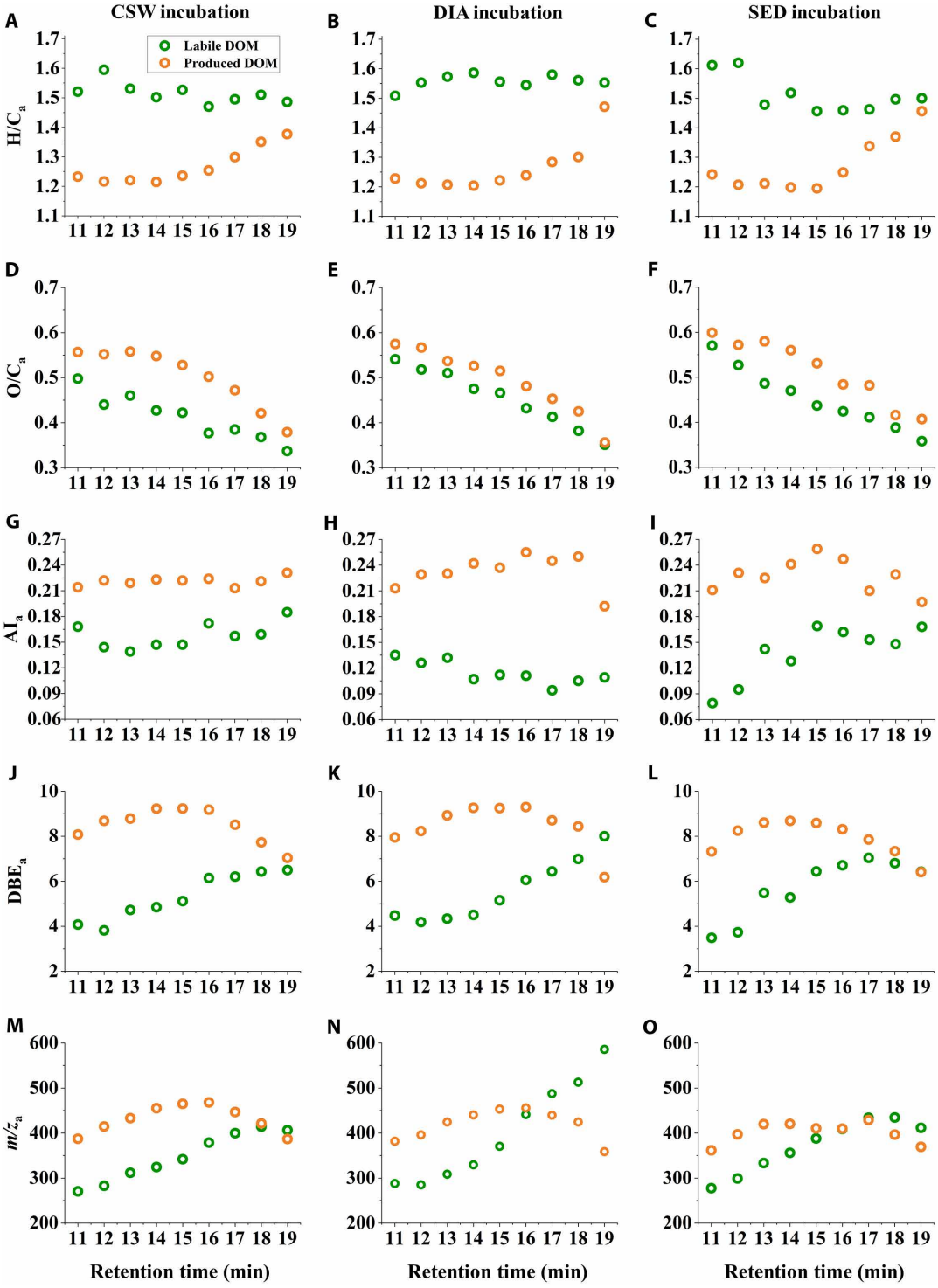

Fig. 3. Bulk chemical characteristics of labile and produced DOM in the CSW, DIA, and SED incubations. DOM formulae uniquely identified in each incubation within the same LC segments on days 0 and 90 were classified as labile and produced DOM, respectively. The average values of key chemical properties were calculated for labile and produced DOM in each LC segment, including (**A** to **C**) H/C_a, (**D** to **F**) O/C_a, (**G** to **I**) AI_a, (**J** to **L**) DBE_a, and (**M** to **O**) m/z_a, for the CSW, DIA, and SED incubations, respectively.

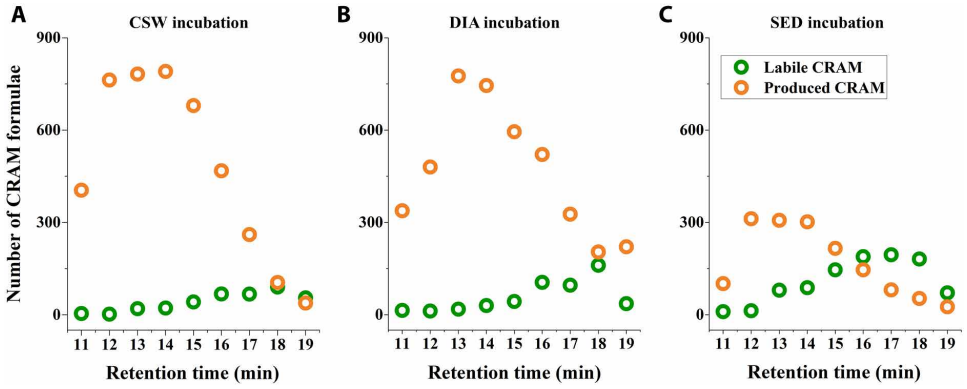

Fig. 4. Molecular formula counts of microbially labile and microbially produced CRAM from incubation experiments. In each LC segment of the CSW (**A**), DIA (**B**), and SED (**C**) incubations, CRAM formulae uniquely identified on days 0 and 90 were classified as labile and produced, respectively.

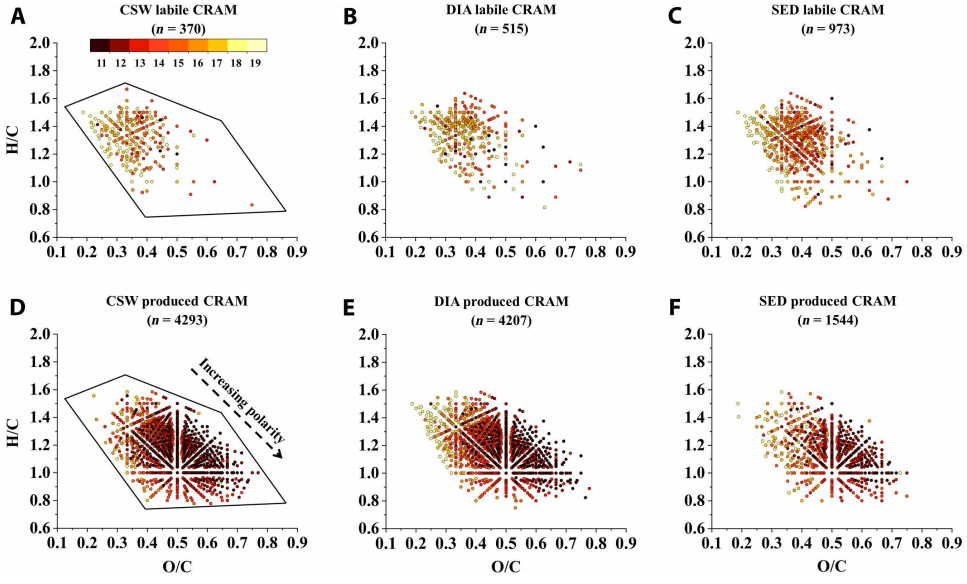

Fig. 5. Van Krevelen diagrams illustrating microbial transformation of CRAM. The microbially labile (**A** to **C**) and microbially produced (**D** to **F**) CRAM in each incubation were indicated with molecular polarity. Color gradients [see the scale in (A)] correspond to LC elution retention times. In each panel, the number of displayed formulae represents the total count of assigned CRAM molecular formulae summed across the nine LC segments.

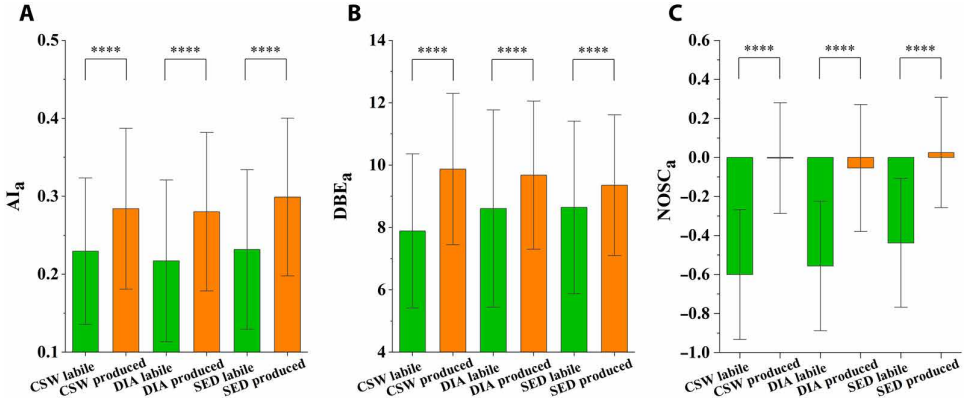

Fig. 6. Distinct molecular characteristics of microbially labile and microbially produced CRAM. Average AI_a (**A**), DBE_a (**B**), and $NOSC_a$ (**C**) values of microbially labile and microbially produced CRAM formulae (as shown in Fig. 5) for each of the CSW, DIA, and SED incubations. Statistical significance was determined using a *t* test (****$P < 0.0001$).

overall polarity, thereby enhancing their biological recalcitrance. In addition, the produced CRAM formulae were enriched in nitrogen and depleted in sulfur and phosphorus content (fig. S11). This chemical modification likely contributes to the increased recalcitrance of CRAM (*8*, *62*) as nitrogen atoms may form stronger chemical bonds in their chemical structures, potentially as aromatic heterocyclic nitrogen (*63*, *64*).

To further consolidate the biorecalcitrance of labile and produced CRAM, we identified 63 and 684 commonly labile and commonly produced CRAM formulae, respectively, across all LC segments from the three incubations (Fig. 7, A and B). We assumed that refractory CRAM should resist rapid degradation and therefore persist in natural seawaters. To evaluate this, we calculated the frequency of detection of the commonly labile and commonly produced CRAM formulae in a synthesized global seawater DOM dataset, comprising 1485 samples (fig. S12 and table S1), to examine their persistence. The meridional distribution of the frequency of detection of these commonly labile and commonly produced CRAM revealed their approximate presence across different oceanic provinces (Fig. 7, C and D). On average, the commonly labile and commonly produced CRAM formulae were present in 37.9 ± 9.7% (means ± SD) and 86.6 ± 5.9% of the 1485 DOM samples, respectively (Fig. 7, C and D). The significantly higher presence of produced CRAM compared to labile CRAM ($P < 0.0001$; *t* test) confirms that the commonly labile CRAM formulae are less likely to persist on ocean turnover time scales. In contrast, the commonly produced CRAM appear to have undergone microbial reworking during the incubation period, exhibit greater resistance to rapid degradation, and are thus more likely to persist in seawater. These findings underscore the critical role of microbial transformation in creating RDOM, enabling its persistence and potential accumulation in certain marine environments (*23*).

This presence analysis of LC-FT-ICR-MS–identified CRAM in our synthesized DI-FT-ICR-MS DOM dataset could overestimate the presences of both commonly labile and commonly produced CRAM in natural seawaters. This potential overestimation arises because LC-FT-ICR-MS detects DOM isomer clusters (*43*, *65*), whereas DI-FT-ICR-MS lacks this capability. In addition, the results of the microbial incubations, conducted under controlled laboratory conditions with a limited range of substrates, were preliminarily extrapolated to areas and water depths with varying temperatures, microbial community structures, and DOM compositions. Nonetheless, our experimental results demonstrate a significant difference ($P < 0.0001$) in the frequency of detection between commonly labile and commonly produced CRAM in the dataset (Fig. 7, C and D). This calculation provides a foundation for future studies to further investigate the global persistence of microbially modified CRAM. It is also worth noting that this study excluded a subset of CRAM formulae that persisted throughout the 90-day incubation period. In contrast to the identification of labile and produced CRAM, which was based solely on their presence at the start and end of the incubation, persistent CRAM formulae exhibited dynamic changes in intensity due to microbial utilization and production (*26*). Their isomeric diversity and composition are likely complex and warrant a dedicated, independent investigation. To maintain the focus and simplicity of the current study, we concentrated on labile and produced DOM to explore the intrinsic relationship between CRAM bioavailability and molecular polarity. The role of isomeric diversity in DOM bioavailability and related dynamics will be addressed in an ongoing study as the LC-FT-ICR-MS methodology shows promise in distinguishing certain DOM isomer clusters within complex DOM mixtures (*43*, *65*, *66*).

In conclusion, this study introduced the application of polarity-based LC-FT-ICR-MS in microbial incubation experiments, revealing

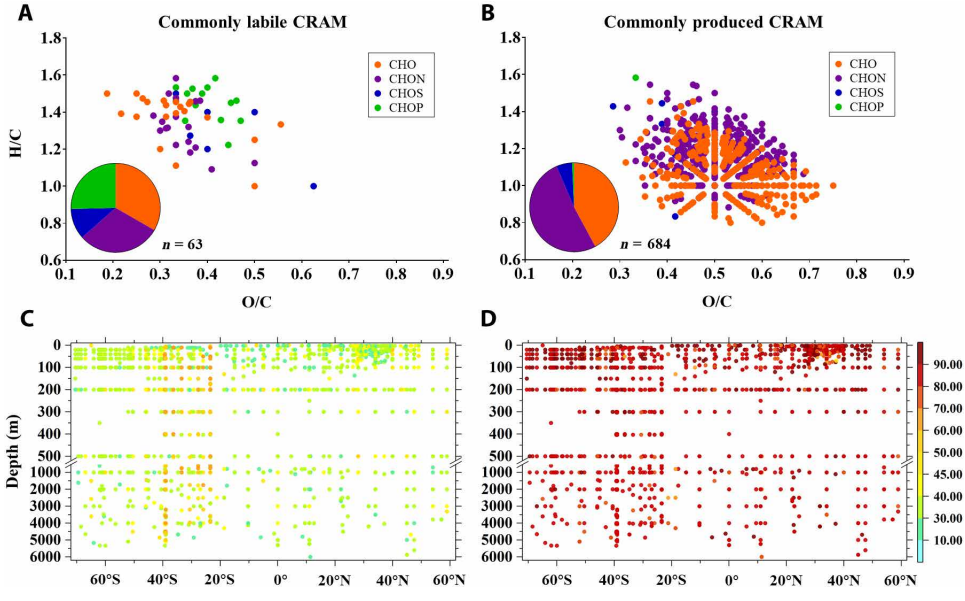

Fig. 7. Molecular characteristics of commonly labile and commonly produced CRAM formulae and their meridional distribution of detection frequency in the global DOM dataset (see fig. S12). van Krevelen diagrams and relative abundances of compound classes (CHO-, CHON-, CHOS-, and CHOP-containing molecules) for the commonly labile (**A**) and commonly produced (**B**) CRAM across the three incubations, respectively. Meridional distribution of frequency of detection for the commonly labile (**C**) and commonly produced (**D**) CRAM, respectively. The color bar in (C) and (D) represents the frequency of detection (%) of these CRAM groups across individual DOM samples in the global dataset. We calculated the detection frequency by first counting the commonly labile ($n = 63$) or commonly produced ($n = 684$) CRAM formulae in each DOM sample and then dividing these counts by their respective totals (63 or 684) to obtain percentages.

that microbes preferentially used lower-polarity SPE-DOM and produced higher-polarity DOM compounds. The microbially produced DOM exhibited characteristics of biological recalcitrance, suggesting that SPE-DOM bioavailability is intrinsically linked to its molecular polarity. We also demonstrated that the widely referred RDOM proxy, CRAM, comprise various molecules with varying degrees of biological recalcitrance. Specifically, CRAM with lower oxidation states and contributions of aromatic structures and nitrogen-containing groups were more likely to be preferentially used or transformed by heterotrophic microbes. These compounds were typically eluted later in online countergradient LC operations, indicating their low polarity. Conversely, microbial reworking increased the oxidation state, aromatic structures, and nitrogen-heteroatom content of CRAM, along with their polarity, enhancing their biological recalcitrance and persistence in natural seawaters, albeit to a limited extent. This finding suggests that CRAM represent a continuum of reactivity rather than a distinct class, similar to the behavior of bulk oceanic DOM (*11*, *12*). This calls into question the practice of categorizing CRAM as an RDOM proxy solely based on ultrahigh-resolution mass spectrometry, without careful consideration. It is important to note that, in the original study defining CRAM from ultrafiltered DOM (*22*), the researchers characterized this material using a combination of ultrahigh-resolution mass spectrometry and high-field nuclear magnetic resonance spectroscopy (*22*). These researchers have consistently applied these two complementary analytical tools to define CRAM, whether derived from ultrafiltered or SPE-DOM (*5*, *31*, *67*).

In addition, the molecular composition of nonretained DOM leached from absorbents commonly used in solid phase extraction (e.g., Agilent Bound Elut-PPL and C-18) could vary among samples (*68*, *69*). The bioavailability of this nonretained DOM fraction remains uncertain, especially as a recent study has found that hydrophilic freshwater DOM compounds can be highly biolabile (*45*). Thus, our current understanding of the refractory nature of the bulk marine DOM pool is still incomplete. Recently, a direct analysis of natural seawater DOM using LC-FT-ICR-MS has been developed (*65*). This method requires only a small volume of seawater and can provide molecular composition data without the need for DOM extraction, making it a promising tool for investigating polar DOM compounds excluded by traditional solid phase extraction approach. With the continued advancement of analytical methodologies, the enigmatic refractory nature and isomeric complexity of marine DOM, the two major conundrums in marine DOM biogeochemistry, may soon be resolved.

MATERIALS AND METHODS

Incubation experiment setup

Before the laboratory incubation, a coastal surface seawater sample was collected near Xiamen Island (24°30′N, 118°14′E) in May 2019. The seawater was filtered through 3.0-μm polycarbonate filters (Millipore, prerinsed with 10 liters of Milli-Q water) to obtain filtrates containing a free-living prokaryotic community and autochthonous DOM. The filtrates were designated as the CSW treatment. Additional treatments were prepared by amending the CSW filtrates with intracellular organic matter from a diatom strain *Thalassiosira pseudonana* CCMP1335 and coastal sediment-derived DOM; for details, see (*26*). As a result, the incubation experiments included a natural seawater treatment (CSW) and two treatments amended with exogenous organic substrates (DIA and SED). The incubations were conducted in a dark, temperature-controlled room (~20°C) for 90 days. The initial total organic carbon concentration in the CSW incubation was ~89 μmol C liter^{-1}, which decreased to ~76 μmol C liter^{-1} by the end of the incubation. Total organic carbon concentrations in the DIA and SED treatments showed sharper declines, dropping from ~535 to ~111 μmol C liter^{-1} and from ~292 to ~91 μmol C liter^{-1}, respectively. Samples analyzed in this study were previously measured using a 9.4-T Bruker Apex Ultra FT-ICR mass spectrometer in direct infusion. Details on the experimental setup, DI-FT-ICR-MS results, bacterial abundance, and organic carbon concentration variations are available in (*26*).

Measurement of the DOM extracts using LC-FT-ICR-MS

DOM from CSW, DIA, and SED incubations was obtained via solid phase extraction using 200-mg styrene divinyl benzene copolymer cartridges (Bond Elut PPL, Agilent) on days 0 and 90, following the protocol of Dittmar *et al.* (*70*). The DOM extraction efficiency ranged from 38 to 52%, similar to the range reported by Dittmar *et al.* (*70*). Further experimental details were described by Lian *et al.* (*26*). Before LC-FT-ICR-MS analysis, the SPE-DOM was adjusted to a dissolved organic carbon concentration of ~10 mg C liter^{-1} to facilitate semi-quantitative DOM compositional comparison across samples. An FT-ICR mass spectrometer (with 12-T refrigerated actively shielded superconducting magnet and dynamically harmonized ICR cell, solariX XR, Bruker Daltonics, Billerica, MA, USA) coupled with LC (Fig. 1) as outlined by Han *et al.* (*43*) was used.

Separation of DOM was performed on an UltiMate 3000RS UHPLC system (Thermo Fisher Scientific) equipped with binary pump (HPG-3200RS), column oven (TCC-3000RS), autosampler (WPS-3000TRS), and diode array detector (DAD-3000RS). The LC system was equipped with a reversed-phase polar end-capped C18 column (ACQUITY HSS T3, 1.8 μm, 100 Å, 150 mm by 3 mm, Waters, Milford, MA) and a guard column (ACQUITY UPLC HSS T3 VanGuard Precolumn, 100 Å, 1.8 μm, 2.1 mm by 5 mm). Ultrapure water (Milli-Q system, Merck, Germany) and LC-MS-grade methanol (Biosolve, Netherlands) were used as mobile phases A and B. Formic acid (0.05%) was added to both eluents. The aqueous eluent was adjusted to pH 3.0 with ammonium hydroxide, and the same volume of ammonium hydroxide was added to eluent B. The eluent gradient started at 0.5 min and linearly increased from 0 to 100% methanol within 14 min. A second HPLC pump (LPG-3400SD) was used to add a postcolumn flow (0.2 ml/min). A gradient was applied to reverse the gradient of the first pump at the column outlet using the same solvents (A: methanol and B: ultrapure water) but without buffer addition.

For the FT-ICR-MS measurement following the LC separation, an electrospray ionization source (Apollo II, Bruker Daltonics Inc., USA) was used in negative mode (capillary voltage: 3.9 kV, nebulizer gas pressure: 1.0 bar, dry gas temperature: 200°C, and dry gas flow rate: 4.0 liters/min) (*43*). Mass spectra for LC-FT-ICR-MS measurements were acquired in broadband *m/z* of 150~1000 with a transient size of 2 M Word and full profile magnitude mode. Lock masses (*m/z* of 150~600) were used to compensate mass shifts during LC acquisition. A total of 834 scans were recorded between 11- and 19-min retention time for each LC-FT-ICR-MS measurement because this retention time range showed the maximum elution of DOM according to the total ion chromatogram.

LC-FT-ICR-MS data processing

LC-FT-ICR-MS spectra were split and averaged using the Data Analysis software (Bruker Daltonics version 6.0). Mass spectra within

1-min retention time intervals were averaged (resulting in nine distinct retention time segments; Fig. 1) and calibrated using known *m/z* values of the Suwannee River Fulvic Acid reference natural organic matter (International Humic Substances Society, USA) via an in-house web-based tool (Lambda-Miner) (*71*). Peak picking was performed with a signal-to-noise ratio threshold of >4 and a mass accuracy of <1 ppm (parts per million) for molecular formula assignment (*72*). Formulae were assigned to the calibrated mass data following Yi *et al.* (*73*). A molecular formula calculator generated matching formulae according to elemental combinations of $^{12}C_{1-60}$, $^{13}C_{0-1}$, $^{1}H_{1-120}$, $^{14}N_{0-3}$, $^{15}N_{0-1}$, $^{16}O_{0-30}$, $^{18}O_{0-1}$, $^{32}S_{0-2}$, $^{34}S_{0-1}$, and $^{31}P_{0-1}$. All assigned DOM formulae had to meet other basic chemical criteria: (i) the number of H atoms should be at least 1/3 that of C atoms and cannot exceed 2C + N + 2; (ii) the sum of H and N atoms must be even (the "nitrogen rule"); and (iii) the O/C ratio should not exceed 1.5. Isotopologs were excluded from further analyses.

Averages of H/C_a, O/C_a, m/z_a, AI_a, DBE_a, and $NOSC_a$ were calculated for each segment of the LC-FT-ICR-MS measurements (*60*, *61*, *74*). These indices have been widely applied to evaluate bioavailability of bulk DOM samples (*49*). Within each LC segment of every incubation experiment (CSW, DIA, and SED), we classified molecular formulae exclusively present in the 0-day incubation as microbially labile DOM, and those exclusively present in the 90-day incubation as microbially produced DOM, with both categories containing CRAM. CRAM molecular formulae were assigned based on an empirical criterion: (DBE/C = 0.30 to 0.68, DBE/H = 0.20 to 0.95, and DBE/O = 0.77 to 1.75) (*22*). In addition, we compiled a global seawater DOM dataset to assess the frequency of detection of the commonly labile and commonly produced CRAM formulae identified in incubations. This dataset included 1485 DOM samples, with 172 measured using a single FT-ICR-MS instrument following a consistent protocol (orange circles in fig. S12) (*75*) and 1313 samples obtained from the literature sources (purple circles in fig. S12) (*11*, *12*, *76*–*79*). We gratefully acknowledge the contributions of these studies. Detailed information regarding the dataset's composition is provided in table S1. To calculate the detection frequency, we first determined the number of commonly labile ($n = 63$) or commonly produced ($n = 684$) CRAM formulae in each DOM sample and then divided these counts by their respective totals (63 or 684) to obtain percentages.

Supplementary Materials

This PDF file includes:

Figs. S1 to S12
Table S1
References

REFERENCES AND NOTES

1. T. Dittmar, S. T. Lennartz, H. Buck-Wiese, D. A. Hansell, C. Santinelli, C. Vanni, B. Blasius, J.-H. Hehemann, Enigmatic persistence of dissolved organic matter in the ocean. *Nat. Rev. Earth Environ.* **2**, 570–583 (2021).
2. M. A. Moran, E. B. Kujawinski, W. F. Schroer, S. A. Amin, N. R. Bates, E. M. Bertrand, R. Braakman, C. T. Brown, M. W. Covert, S. C. Doney, S. T. Dyhrman, A. S. Edison, A. M. Eren, N. M. Levine, L. Li, A. C. Ross, M. A. Saito, A. E. Santoro, D. Segre, A. Shade, M. B. Sullivan, A. Vardi, Microbial metabolites in the marine carbon cycle. *Nat. Microbiol.* **7**, 508–523 (2022).
3. D. A. Hansell, Recalcitrant dissolved organic carbon fractions. *Ann. Rev. Mar. Sci.* **5**, 421–445 (2013).
4. R. LaBrie, B. Pequin, N. F. St-Gelais, I. Yashayaev, J. Cherrier, Y. Gelinas, F. Guillemette, D. C. Podgorski, R. G. M. Spencer, L. Tremblay, R. Maranger, Deep ocean microbial communities produce more stable dissolved organic matter through the succession of rare prokaryotes. *Sci. Adv.* **8**, eabn0035 (2022).
5. O. J. Lechtenfeld, N. Hertkorn, Y. Shen, M. Witt, R. Benner, Marine sequestration of carbon in bacterial metabolites. *Nat. Commun.* **6**, 6711 (2015).
6. H. Osterholz, J. Niggemann, H. A. Giebel, M. Simon, T. Dittmar, Inefficient microbial production of refractory dissolved organic matter in the ocean. *Nat. Commun.* **6**, 7422 (2015).
7. B. P. Koch, G. Kattner, M. Witt, U. Passow, Molecular insights into the microbial formation of marine dissolved organic matter: Recalcitrant or labile? *Biogeosciences* **11**, 4173–4190 (2014).
8. K. B. Ksionzek, O. J. Lechtenfeld, S. L. McCallister, P. Schmitt-Kopplin, J. K. Geuer, W. Geibert, B. P. Koch, Dissolved organic sulfur in the ocean: Biogeochemistry of a petagram inventory. *Science* **354**, 456–459 (2016).
9. M. Zark, T. Dittmar, Universal molecular structures in natural dissolved organic matter. *Nat. Commun.* **9**, 3178 (2018).
10. P. M. Medeiros, M. Seidel, L. C. Powers, T. Dittmar, D. A. Hansell, W. L. Miller, Dissolved organic matter composition and photochemical transformations in the northern North Pacific Ocean. *Geophys. Res. Lett.* **42**, 863–870 (2015).
11. O. J. Lechtenfeld, G. Kattner, R. Flerus, S. L. McCallister, P. Schmitt-Kopplin, B. P. Koch, Molecular transformation and degradation of refractory dissolved organic matter in the Atlantic and Southern Ocean. *Geochim. Cosmochim. Acta* **126**, 321–337 (2014).
12. R. Flerus, O. J. Lechtenfeld, B. P. Koch, S. L. McCallister, P. Schmitt-Kopplin, R. Benner, K. Kaiser, G. Kattner, A molecular perspective on the ageing of marine dissolved organic matter. *Biogeosciences* **9**, 1935–1955 (2012).
13. X. Zheng, R. Cai, H. Yao, X. Zhuo, C. He, Q. Zheng, Q. Shi, N. Jiao, Experimental insight into the enigmatic persistence of marine refractory dissolved organic matter. *Environ. Sci. Technol.* **56**, 17420–17429 (2022).
14. M. Seidel, S. P. B. Vemulapalli, D. Mathieu, T. Dittmar, Marine dissolved organic matter shares thousands of molecular formulae yet differs structurally across major water masses. *Environ. Sci. Technol.* **56**, 3758–3769 (2022).
15. J. M. Arrieta, E. Mayol, R. L. Hansman, G. J. Herndl, T. Dittmar, C. M. Duarte, Dilution limits dissolved organic carbon utilization in the deep ocean. *Science* **348**, 331–333 (2015).
16. J. A. Hawkes, P. E. Rossel, A. Stubbins, D. Butterfield, D. P. Connelly, E. P. Achterberg, A. Koschinsky, V. Chavagnac, C. T. Hansen, W. Bach, T. Dittmar, Efficient removal of recalcitrant deep-ocean dissolved organic matter during hydrothermal circulation. *Nat. Geosci.* **8**, 856–860 (2015).
17. E. A. Hawkes, A. Patrlarca, P. J. R. Sjoberg, L. J. Tranvik, J. Bergquist, Extreme isomeric complexity of dissolved organic matter found across aquatic environments. *Limnol. Oceanogr. Lett.* **3**, 21–30 (2018).
18. R. M. Boiteau, Y. E. Corilo, W. R. Kew, C. Dewey, M. C. A. Rodriguez, C. A. Carlson, T. M. Conway, Relating molecular properties to the persistence of marine dissolved organic matter with liquid chromatography-ultrahigh-resolution mass spectrometry. *Environ. Sci. Technol.* **58**, 3267–3277 (2024).
19. T. S. Catala, S. Shorte, T. Dittmar, Marine dissolved organic matter: A vast and unexplored molecular space. *Appl. Microbiol. Biotechnol.* **105**, 7225–7239 (2021).
20. P. F. Sexton, R. D. Norris, P. A. Wilson, P. L. Heiko, W. Thomas, R. H. Ursula, C. T. Bolton, G. Samantha, Eocene global warming events driven by ventilation of oceanic dissolved organic carbon. *Nature* **471**, 349–352 (2011).
21. D. H. Rothman, J. M. Hayes, R. E. Summons, Dynamics of the Neoproterozoic carbon cycle. *Proc. Natl. Acad. Sci. U.S.A.* **100**, 8124–8129 (2003).
22. N. Hertkorn, R. Benner, M. Frommberger, P. Schmitt-Kopplin, M. Witt, K. Kaiser, A. Kettrup, J. I. Hedges, Characterization of a major refractory component of marine dissolved organic matter. *Geochim. Cosmochim. Acta* **70**, 2990–3010 (2006).
23. N. Jiao, R. Cai, Q. Zheng, K. Tang, J. Liu, F. Jiao, D. Wallace, F. Chen, C. Li, R. Amann, R. Benner, F. Azam, Unveiling the enigma of refractory carbon in the ocean. *Natl. Sci. Rev.* **5**, 459–463 (2018).
24. H. Li, Z. Zhang, T. Xiong, K. Tang, C. He, Q. Shi, N. Jiao, Y. Zhang, Carbon sequestration in the form of recalcitrant dissolved organic carbon in a seaweed (kelp) farming environment. *Environ. Sci. Technol.* **56**, 9112–9122 (2022).
25. X. Feng, H. Li, Z. Zhang, T. Xiong, X. Shi, C. He, Q. Shi, N. Jiao, Y. Zhang, Microbial-mediated contribution of kelp detritus to different forms of oceanic carbon sequestration. *Ecol. Indic.* **142**, 109186 (2022).
26. J. Lian, X. Zheng, X. Zhuo, Y.-L. Chen, C. He, Q. Zheng, T.-H. Lin, J. Sun, W. Guo, Q. Shi, N. Jiao, R. Cai, Microbial transformation of distinct exogenous substrates into analogous composition of recalcitrant dissolved organic matter. *Environ. Microbiol.* **23**, 2389–2403 (2021).
27. D. C. Podgorski, P. Zito, A. M. Kellerman, B. A. Bekins, I. M. Cozzarelli, D. F. Smith, X. Cao, K. Schmidt-Rohr, S. Wagner, A. Stubbins, R. G. M. Spencer, Hydrocarbons to carboxyl-rich alicyclic molecules: A continuum model to describe biodegradation of petroleum-derived dissolved organic matter in contaminated groundwater plumes. *J. Hazard. Mater.* **402**, 123998 (2021).
28. P. Li, J. Tao, J. Lin, C. He, Q. Shi, X. Li, C. Zhang, Stratification of dissolved organic matter in the upper 2000 m water column at the Mariana Trench. *Sci. Total Environ.* **668**, 1222–1231 (2019).

29. Y. Liu, X. Liu, Y. Long, Y. Wen, C. Ma, J. Sun, Variations in dissolved organic matter chemistry on a vertical scale in the eastern Indian Ocean. *Water Res.* **232**, 119674 (2023).
30. T. A. B. Broek, B. D. Walker, T. P. Guilderson, J. S. Vaughn, H. E. Mason, M. D. McCarthy, Low molecular weight dissolved organic carbon: Aging, compositional changes, and selective utilization during global ocean circulation. *Global Biogeochem. Cycles* **34**, e2020GB006547 (2020).
31. N. Hertkorn, M. Harir, B. P. Koch, B. Michalke, P. Schmitt-Kopplin, High-field NMR spectroscopy and FTICR mass spectrometry: Powerful discovery tools for the molecular level characterization of marine dissolved organic matter. *Biogeosciences* **10**, 1583–1624 (2013).
32. P. Jiang, H. Chen, Z. Liu, X. Li, Comparing the isotopic and molecular composition of dissolved organic carbon between the oligotrophic South China Sea and the adjacent North Pacific Ocean: Signals of biodegradation, conservative mixing, and terrestrial input. *Mar. Chem.* **257**, 104331 (2023).
33. C. Zhao, Y. Hou, Y. Wang, P. Li, C. He, Q. Shi, Y. Yi, D. He, Unraveling the photochemical reactivity of dissolved organic matter in the Yangtze river estuary: Integrating incubations with field observations. *Water Res.* **245**, 120638 (2023).
34. B. Bayer, R. L. Hansman, M. J. Bittner, B. E. Noriega-Ortega, J. Niggemann, T. Dittmar, G. J. Herndl, Ammonia-oxidizing archaea release a suite of organic compounds potentially fueling prokaryotic heterotrophy in the ocean. *Environ. Microbiol.* **21**, 4062–4075 (2019).
35. S. Liu, R. Parsons, K. Opalk, N. Baetge, S. Giovannoni, L. M. Bolanos, E. B. Kujawinski, K. Longnecker, Y. Lu, E. Halewood, C. A. Carlson, Different carboxyl-rich alicyclic molecules proxy compounds select distinct bacterioplankton for oxidation of dissolved organic matter in the mesopelagic Sargasso Sea. *Limnol. Oceanogr.* **65**, 1532–1553 (2020).
36. K. McKee, H. Abdulla, L. O'Reilly, B. D. Walker, Cycling of labile and recalcitrant carboxyl-rich alicyclic molecules and carbohydrates in Baffin Bay. *Nat. Commun.* **15**, 8735 (2024).
37. C. Patriarca, J. Bergquist, P. J. R. Sjoberg, L. Tranvik, J. A. Hawkes, Online HPLC-ESI-HRMS method for the analysis and comparison of different dissolved organic matter samples. *Environ. Sci. Technol.* **52**, 2091–2099 (2018).
38. Y. Qi, C. Ma, S. Chen, J. Ge, Q. Hu, S.-L. Li, D. A. Volmer, P. Fu, Online liquid chromatography and FT-ICR MS enable advanced separation and profiling of organosulfates in dissolved organic matter. *ACS ES&T Water* **1**, 1975–1982 (2021).
39. D. Kim, S. Kim, S. Son, M.-J. Jung, S. Kim, Application of online liquid chromatography 7 T FT-ICR mass spectrometer equipped with quadrupolar detection for analysis of natural organic matter. *Anal. Chem.* **91**, 7690–7697 (2019).
40. S. Papadopoulos Lambidis, T. Schramm, K. Steuer-Lodd, S. Farrell, P. Stincone, R. Schmid, I. Koester, R. Torres, T. Dittmar, L. Aluwihare, C. Simon, D. Petras, Two-dimensional liquid chromatography tandem mass spectrometry untangles the deep metabolome of marine dissolved organic matter. *Environ. Sci. Technol.* **58**, 19289–19304 (2024).
41. Y. Li, C. He, Y. Zhang, Q. Shi, Online LC-Orbitrap MS method for the rapid molecular characterization of dissolved organic matter. *Rapid Commun. Mass Spectrom.* **38**, e9885 (2024).
42. S. L. Felgate, E. Jakobsson, A. B. Subieta, L. J. Tranvik, J. A. Hawkes, Combined quantification and characterization of dissolved organic matter by liquid chromatography-mass spectrometry using charged aerosol detection. *J. Am. Soc. Mass Spectrom.* **35**, 2910–2917 (2024).
43. L. Han, J. Kaesler, C. Peng, T. Reemtsma, O. J. Lechtenfeld, Online counter gradient LC-FT-ICR-MS enables detection of highly polar natural organic matter fractions. *Anal. Chem.* **93**, 1740–1748 (2021).
44. E. Jennings, A. Kremser, L. Han, T. Reemtsma, O. J. Lechtenfeld, Discovery of polar ozonation byproducts via direct Injection of effluent organic matter with online LC-FT-ICR-MS. *Environ. Sci. Technol.* **56**, 1894–1904 (2022).
45. C. Grasset, M. Groeneveld, L. J. Tranvik, L. P. Robertson, J. A. Hawkes, Hydrophilic species are the most biodegradable components of freshwater dissolved organic matter. *Environ. Sci. Technol.* **57**, 13463–13472 (2023).
46. P. Li, W. Liang, Y. Zhou, Y. Yi, C. He, Q. Shi, D. He, Hypoxia diversifies molecular composition of dissolved organic matter and enhances preservation of terrestrial organic carbon in the Yangtze River Estuary. *Sci. Total Environ.* **906**, 167661 (2024).
47. N. Kamjunke, P. Herzsprung, W. V. Tümpling, O. J. Lechtenfeld, Photochemical and microbial degradation of deadwood leachate. *J. Geophys. Res. Biogeosci.* **129**, e2024JG008184 (2024).
48. E. C. Freeman, E. J. S. Emilson, T. Dittmar, L. P. P. Braga, C. E. Emilson, T. Goldhammer, C. Martineau, G. Singer, A. J. Tanentzap, Universal microbial reworking of dissolved organic matter along environmental gradients. *Nat. Commun.* **15**, 187 (2024).
49. R. Cai, N. Jiao, Recalcitrant dissolved organic matter and its major production and removal processes in the ocean. *Deep Sea Res. 1 Oceanogr. Res. Pap.* **191**, 103922 (2023).
50. R. Cai, W. Zhou, C. He, K. Tang, W. Guo, Q. Shi, M. Gonsior, N. Jiao, Microbial processing of sediment-derived dissolved organic matter: Implications for Its subsequent biogeochemical cycling in overlying seawater. *J. Geophys. Res. Biogeosci.* **124**, 3479–3490 (2019).
51. A. Maria Martinez-Perez, H. Osterholz, M. Nieto-Cid, M. Alvarez, T. Dittmar, X. Anton Alvarez-Salgado, Molecular composition of dissolved organic matter in the Mediterranean Sea. *Limnol. Oceanogr.* **62**, 2699–2712 (2017).
52. R. LaBrie, J.-F. Lapierre, R. Maranger, Contrasting patterns of labile and semilabile dissolved organic carbon from continental waters to the open ocean. *J. Geophys. Res. Biogeosci.* **125**, e2019JG005300 (2020).
53. H. Chen, A. Stubbins, E. M. Perdue, N. W. Green, J. R. Helms, K. Mopper, P. G. Hatcher, Ultrahigh resolution mass spectrometric differentiation of dissolved organic matter isolated by coupled reverse osmosis-electrodialysis from various major oceanic water masses. *Mar. Chem.* **164**, 48–59 (2014).
54. M. Yang, P. D. Nightingale, R. Beale, P. S. Liss, B. Blomquist, C. Fairall, Atmospheric deposition of methanol over the Atlantic Ocean. *Proc. Natl. Acad. Sci. U.S.A.* **110**, 20034–20039 (2013).
55. W. Deng, L. Peng, N. Jiao, Y. Zhang, Differential incorporation of one-carbon substrates among microbial populations identified by stable isotope probing from the estuary to South China Sea. *Sci. Rep.* **8**, 15378 (2018).
56. Y. Shen, C. G. Fichot, S.-K. Liang, R. Benner, Biological hot spots and the accumulation of marine dissolved organic matter in a highly productive ocean margin. *Limnol. Oceanogr.* **61**, 1287–1300 (2016).
57. H. Osterholz, G. Singer, B. Wemheuer, R. Daniel, M. Simon, J. Niggemann, T. Dittmar, Deciphering associations between dissolved organic molecules and bacterial communities in a pelagic marine system. *ISME J.* **10**, 1717–1730 (2016).
58. J. A. Hawkes, Electrospray ionisation suppression in aquatic dissolved organic matter studies—Investigation via liquid chromatography-mass spectrometry. *Org. Geochem.* **196**, 104852 (2024).
59. Z. Liu, R. Cai, Y.-L. Chen, X. Zhuo, C. He, Q. Zheng, D. He, Q. Shi, N. Jiao, Direct production of bio-recalcitrant carboxyl-rich alicyclic molecules evidenced in a bacterium-induced steroid degradation experiment. *Microbiol. Spectr.* **11**, e04693-22 (2023).
60. B. P. Koch, T. Dittmar, From mass to structure: An aromaticity index for high-resolution mass data of natural organic matter. *Rapid Commun. Mass Spectrom.* **20**, 926–932 (2006).
61. D. E. LaRowe, P. Van Cappellen, Degradation of natural organic matter: A thermodynamic analysis. *Geochim. Cosmochim. Acta* **75**, 2030–2042 (2011).
62. Z. Yan, Y. Xin, X. Zhong, Y. Yi, P. Li, Y. Wang, Y. Zhou, Y. He, C. He, Q. Shi, W. Xu, D. He, Evolution of dissolved organic nitrogen chemistry during transportation to the marginal sea: Insights from nitrogen isotope and molecular composition analyses. *Water Res.* **249**, 120942 (2023).
63. T. A. B. Broek, M. D. McCarthy, H. L. Ianiri, J. S. Vaughn, H. E. Mason, A. N. Knapp, Dominant heterocyclic composition of dissolved organic nitrogen in the ocean: A new paradigm for cycling and persistence. *Proc. Natl. Acad. Sci. U.S.A.* **120**, e2305763120 (2023).
64. H. L. Ianiri, H. E. Mason, T. A. B. Broek, M. D. McCarthy, Improved solid-state 13C and 15N NMR reveals fundamental compositional divide between refractory dissolved organic carbon and nitrogen in the sea. *Geochim. Cosmochim. Acta* **384**, 155–167 (2024).
65. O. J. Lechtenfeld, J. Kaesler, E. K. Jennings, B. P. Koch, Direct analysis of marine dissolved organic matter using LC-FT-ICR MS. *Environ. Sci. Technol.* **58**, 4637–4647 (2024).
66. K. Lu, X. Li, H. Chen, Z. Liu, Constraints on isomers of dissolved organic matter in aquatic environments: Insights from ion mobility mass spectrometry. *Geochim. Cosmochim. Acta* **308**, 353–372 (2021).
67. N. Hertkorn, M. Harir, K. M. Cawley, P. Schmitt-Kopplin, R. Jaffe, Molecular characterization of dissolved organic matter from subtropical wetlands: A comparative study through the analysis of optical properties, NMR and FTICR/MS. *Biogeosciences* **13**, 2257–2277 (2016).
68. X. Kong, T. Jendrossek, K.-U. Ludwichowski, U. Marx, B. P. Koch, Solid-phase extraction of aquatic organic matter: Poading-dependent chemical fractionation and self-assembly. *Environ. Sci. Technol.* **55**, 15495–15504 (2021).
69. Y. Li, M. Harir, J. Uhl, B. Kanawati, M. Lucio, K. S. Smirnov, B. P. Koch, P. Schmitt-Kopplin, N. Hertkorn, How representative are dissolved organic matter (DOM) extracts? A comprehensive study of sorbent selectivity for DOM isolation. *Water Res.* **116**, 316–323 (2017).
70. T. Dittmar, B. Koch, N. Hertkorn, G. Kattner, A simple and efficient method for the solid-phase extraction of dissolved organic matter (SPE-DOM) from seawater. *Limnol. Oceanogr. Methods* **6**, 230–235 (2008).
71. J. Wurz, A. Groß, K. Franze, O. J. Lechtenfeld, "Lambda-Miner: Enhancing reproducible natural organic matter data processing with a semi-automatic web application," *EGU General Assembly 2024*, Vienna, Austria, 14 to 19 April 2024 (Abstract EGU24-15782, 2024); https://doi.org/10.5194/egusphere-egu24-15782.
72. R. Cai, P. Yao, Y. Yi, J. Merder, P. Li, D. He, The hunt for chemical dark matter across a river-to-ocean continuum. *Environ. Sci. Technol.* **58**, 11988–11997 (2024).
73. Y. Yi, C. He, K. Klaproth, J. Merder, P. Li, Y. Qi, P. Fu, S. Li, T. Dittmar, Q. Shi, D. He, Will various interpretation strategies of the same ultrahigh-resolution mass spectrometry data tell different biogeochemical stories? A first assessment based on natural aquatic dissolved organic matter. *Limnol. Oceanogr. Methods* **21**, 320–333 (2023).
74. B. P. Koch, T. Dittmar, From mass to structure: An aromaticity index for high-resolution mass data of natural organic matter (vol. 20, p. 926, 2006). *Rapid Commun. Mass Spectrom.* **30**, 250–250 (2016).

75. C. He, Y. Zhang, Y. Li, X. Zhuo, Y. Li, C. Zhang, Q. Shi, In-house standard method for molecular characterization of dissolved organic matter by FT-ICR Mass Spectrometry. *ACS Omega* **5**, 11730–11736 (2020).
76. H. Osterholz, D. P. A. Kilgour, D. S. Storey, G. Lavik, T. G. Ferdelman, J. Niggemann, T. Dittmar, Accumulation of DOC in the South Pacific Subtropical Gyre from a molecular perspective. *Mar. Chem.* **231**, 103955 (2021).
77. A. M. Kellerman, F. Guillemette, D. C. Podgorski, G. R. Aiken, K. D. Butler, R. G. M. Spencer, Unifying concepts linking dissolved organic matter composition to persistence in aquatic ecosystems. *Environ. Sci. Technol.* **52**, 2538–2548 (2018).
78. T. Riedel, M. Zark, A. V. Vahatalo, J. Niggemann, R. G. M. Spencer, P. J. Hernes, T. Dittmar, Molecular signatures of biogeochemical transformations in dissolved organic matter from ten world rivers. *Front. Earth Sci.* **4**, 85 (2016).
79. S. K. Bercovici, M. Wiemers, T. Dittmar, J. Niggemann, Disentangling biological transformations and photodegradation processes from marine dissolved organic matter composition in the global ocean. *Environ. Sci. Technol.* **57**, 21145–21155 (2023).
80. T. Šantl-Temkiv, K. Finster, T. Dittmar, B. M. Hansen, R. Thyrhaug, N. W. Nielsen, U. G. Karlson, Hailstones: A window into the microbial and chemical inventory of a storm cloud. *PLOS ONE* **8**, e53550 (2013).

Acknowledgments
Funding: This work was supported by the National Natural Science Foundation of China (42222061, 42188102, and U24A20610), Shenzhen-Hong Kong-Macau Science and Technology Program (Category C) (SGDX20230821102400001), grants from the Research Grants Council of the Hong Kong Special Administrative Region, China (AoE/P-601/23-N and 16306623), the Center for Ocean Research in Hong Kong and Macau (CORE), and the Global Ocean Negative Carbon Emissions Program. CORE is a joint research center for ocean research between the Laoshan Laboratory and HKUST. R.C. was supported by the Visiting Fellowship of the State Key Laboratory of Marine Environmental Science at Xiamen University. **Author contributions:** Conceptualization: D.H., R.C., O.J.L., and B.P.K. Methodology: O.J.L., R.C., Y.Y., and D.H. Resources: R.C., D.H., O.J.L., B.P.K., N.J., and Q.Z. Investigation: R.C., O.J.L., D.H, Z.Y., Y.Y., B.P.K., Q.Z., and N.J. Visualization: R.C., D.H., O.J.L., X.C., and N.J. Formal analysis: R.C., Z.Y., D.H., B.P.K., X.C., and N.J. Data curation: R.C., D.H., and B.P.K. Validation: R.C., O.J.L., D.H., B.P.K., and N.J. Supervision: D.H. and O.J.L. Software: O.J.L., Y.Y., R.C., and D.H. Project administration: D.H. and R.C. Funding acquisition: D.H. and N.J. Writing—original draft: R.C. and B.P.K. Writing—review and editing: D.H., O.J.L., B.P.K., R.C., Z.Y., and N.J. **Competing interests:** The authors declare that they have no competing interests. **Data and materials availability:** All data needed to evaluate the conclusions in the paper are present in the paper and/or the Supplementary Materials. The molecular formulae obtained from LC-FT-ICR-MS analysis have been deposited in Zenodo (https://doi.org/10.5281/zenodo.15256601). A subset of DI-FT-ICR-MS data for the global seawater DOM dataset (*76*, *79*) were obtained from PANGAEA [Bercovici et al. (2023); https://doi.org/10.1594/PANGAEA.962747], with additional data of nine samples kindly shared by T. Dittmar, A. M. Kellerman, and R. G. M. Spencer.

Submitted 22 January 2025
Accepted 9 June 2025
Published 11 July 2025
10.1126/sciadv.adw1148

Correction (13 January 2026): The Data and materials availability statement has been updated to acknowledge the following data source related to (*76*, *79*): S. Bercovici, H. Osterholz, M. Wiemers, B. E. Noriega-Ortega, T. Dittmar, J. Niggemann, Dissolved organic matter molecular composition data and supporting metadata for multiple oceanographic cruises with RV SONNE (SO254, SO245, SO248) and RV POLARSTERN (PS79), Bermuda Atlantic Time-series Study and Hawaii Ocean Time-series, PANGAEA (2023); https://doi.org/10.1594/PANGAEA.962747. The PDF and XML have been updated.